Journal of Power Sources 195 (2010) 4923–4927

Contents lists available at ScienceDirect

Journal of Power Sources

journal homepage: www.elsevier.com/locate/jpowsour

Evaluation of $Ba_2(In_{0.8}Ti_{0.2})_2O_{5.2-n}(OH)_{2n}$ as a potential electrolyte material for proton-conducting solid oxide fuel cell

Eric Quarez[a,*], Samuel Noirault[a], Annie Le Gal La Salle[a], Philippe Stevens[b], Olivier Joubert[a]

[a] Institut des Matériaux Jean Rouxel (IMN), Université de Nantes, CNRS, 2, rue de la Houssinière, BP 32229, 44322 Nantes cedex 3, France
[b] EDF R&D, Département LME, Avenue des renardières, 77818 Moret-Sur-Loing, France

ARTICLE INFO

Article history:
Received 9 September 2009
Received in revised form 11 February 2010
Accepted 13 February 2010
Available online 19 February 2010

Keywords:
Titanium substituted barium indate
Fuel cell preparation and testing
Proton conductivity
SOFC

ABSTRACT

Electrochemical measurements of fuel cells based on proton conductor electrolyte $Ba_2(In_{0.8}Ti_{0.2})_2O_{5.2-n}(OH)_{2n}$ and prepared through a tape casting process and a co-pressing of anode-composite powder and electrolyte tape were performed at 500 °C under wet H_2. The varying parameter between the prepared cells was the thickness of the electrolyte that can be controlled during the tape casting process. The maximum power density was obtained for the cell with the thinnest electrolyte (35 μm) and was about 22 mW cm^{-2} with an ohmic resistance about 2 Ω cm^2 at 500 °C.

1. Introduction

For the last couple of years, the development of solid oxide fuel cells based on proton-conducting electrolyte has exploded exponentially [1–46]. The main interest of proton vs. oxygen conduction in fuel cells is the lower operating temperature impacting the life time of the components, the cost of the components required for the operation of the cells (interconnectors, etc.) and the formation of water on the cathode side, which avoids fuel dilution and recycling and reduces risk of destructive anode oxidation even at high current densities. Proton-conducting oxide electrolytes are generally doped perovskites such as doped barium cerate compounds which have drawn the main attention up to now [1–22,25–38,40,42–46]. But these types of materials tend to exhibit high basicity leading to a poor chemical and mechanical stability. In the search of more stable proton-conducting materials for an equivalent proton conductivity level, we investigated materials based on doped barium indate oxide [47–51]. We demonstrated in a recent publication that $Ba_2(In_{1-x}Ti_x)_2O_{5+x}\square_{1-x}$ ($0 \le x \le 0.7$), the so-called BIT*x* phases, incorporate protons by contact with water vapour to form $Ba_2(In_{1-x}Ti_x)_2O_{5+x-n}\square_{1-x-n}(OH)_{2n}$ phases [52]. The best compromise between high proton conductivity level and stability under a wet atmosphere was obtained for $x = 0.2$. The proton conductivity level for this composition was above 1×10^{-3} S cm^{-1} between 400 and 500 °C. In the present article, a fuel cell based on this material was built and tested. Various methods have been utilized to prepare complete solid oxide fuel cells. The most common process starts with the preparation of the half cell with anode and electrolyte components, the cathode being generally deposited afterwards on the electrolyte side as a thin layer. Since the electrolyte thickness has a direct influence on the ohmic resistance of the cell and therefore on its performance, the electrolyte supported technology [4,6–8,19–20,24,41,42] is less and less utilized to the profit of the anode-supported technology [1–3,5,9–18,21–23,25–40,43–46]. Many techniques to prepare anode-supported cells have been reported in the literature [53–55 and references therein]. Among them, two techniques relatively simple to implement and cost-effective, involving a co-pressing of anode and electrolyte materials have attracted our attention. In one technique, anode and electrolyte were in the form of powder [1–3,12,15–18,21,25,27,30,35,40,45,46] and in another technique, both components were prepared by tape casting to produce two different tapes [56]. After co-pressing both constituents in their respective form, the half-cells were co-sintered at high temperature. In the present article, the advantages of both techniques were combined to develop an innovative and new technique based on the co-pressing of an electrolyte tape associated with anode powder. It has the advantage of the tape casting process that permits to control the thickness of the electrolyte and to prepare reproducible uniform surface with large area. It has the advantage of the use of anode powder without organic parts: on account of the presence in large proportion of the anode component in an anode-supported fuel cell, a large amount of polymeric binders and plasticizers will have to be removed during the sintering process,

* Corresponding author. Tel.: +33 2 40 37 39 13; fax: +33 2 40 37 39 95.
E-mail address: Eric.Quarez@cnrs-imn.fr (E. Quarez).

0378-7753/$ – see front matter © 2010 Elsevier B.V. All rights reserved.
doi:10.1016/j.jpowsour.2010.02.030

which may affect, if not controlled, the good contraction process of the sample. In this article, we explain in detail the fabrication of a complete fuel cell and show the results of the electrochemical tests performed on cells functioning at 500 °C under wet hydrogen. Two cells with different electrolyte thicknesses namely 35 and 65 μm have been tested resulting in improved performances and a significant lower ohmic resistance for the cell with the thinnest electrolyte. Only a few proton compounds not based on barium cerate have been studied as electrolyte in SOFC; the work concerning these phases is still in its early stages [23,24,39,41]. The article presents the first investigations concerning the testing of proton-conducting solid oxide fuel cells based on an innovative electrolyte BIT02. The preliminary results obtained show the sustainability of such systems and open the way for further improvements and optimizations.

2. Experimental

2.1. Synthesis

$Ba_2(In_{1-x}Ti_x)_2O_{5+x}\square_{1-x}$ ($x = 0.2$) material was prepared by solid state reaction in air from $BaCO_3$, In_2O_3 and TiO_2 as described earlier in [49]. Stoichiometric mixtures of the reactants, according to the cation stoichiometry of the BITx compound, were ground in mortar and heated at 1200 °C for 24 h. The products were then compacted in pellets and heated at 1350 °C for 24 h. Part of the products was manually ground in mortar and passed through a 100 μm sieve in order to prepare the cermet anode [48] and to carry out the TGA study. To prepare the electrolyte thin film by tape casting, further grinding using a FRITSCH P7 planetary micro-mill during 4 h at 500 rpm was carried out. The particle size distribution of the ball-milled electrolyte powder was measured with a COULTER LS230 instrument.

2.2. Thermogravimetric analyses

Thermal gravimetric analyses of BIT02/NiO composite were performed using a SETARAM microbalance mtb 10-8 under wet Ar/H_2 5(%). Wet air was obtained by passing the gas through a glass tube containing distilled water at 20 °C ($p_{H_2O} = 0.023$ atm).

2.3. X-ray diffraction study

Room temperature XRD data of the TGA residue were obtained using a Brüker "D8 Advance" powder diffractometer operated in Bragg-Brentano reflection geometry with a Cu anode X-ray source, a focusing Ge(1 1 1) primary monochromator (selecting the Cu Kalpha1 radiation) and a 1-D position-sensitive detector ("Vantec" detector).

2.4. SEM characterization

Microstructural features (composition and layers thickness) of the samples were examined by scanning electron microscopy using JEOL JSM 5800 LV recorded with secondary or backscattered electron detector.

2.5. Fuel cells preparation

Three main techniques to assemble anode and electrolyte components have been mostly utilized: the first one deals with the in situ reaction of electrolyte on anode pre-pressed powder [9,10,13,23,29,31–34,38,39,43,44], the second one is based on the co-pressing of anode and electrolyte powders [1–3,12,15–18,21,25,27,30,35,40,45,46], the third one is the electrolyte slurry sprayed onto anode substrate [5,11,14,26,28]. We investigate here a new method of preparation which brings into play the tape casting process and the co-pressing of anode powder and electrolyte tape.

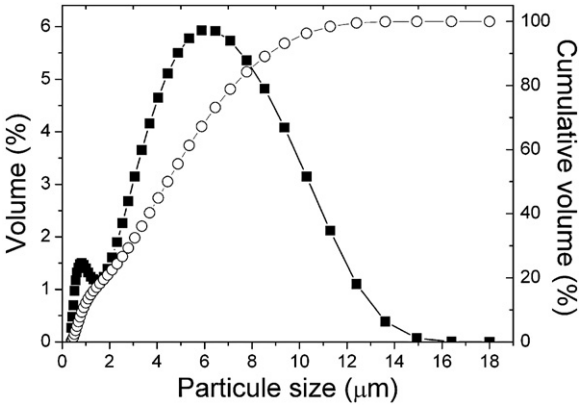

Fig. 1. Particle size distribution of the BIT02 electrolyte powder after micro-milling for 4 h.

The composite powder for anode substrates was prepared by mixing NiO (grain size 0.5–1 μm) and BIT02 powder in weight ratio of 50:50 by manual grinding. In order to maintain interconnected porosity within the sintered sample to facilitate gas diffusion, 7 wt.% sugar powder was added to the composite as pore former.

The particle size distribution analysis shows that the ball-milled BIT02 powder is mainly comprised of particles with size between 0.4 and 12 μm (99%) (Fig. 1). The BIT02 electrolyte film was prepared by tape casting process. The BIT02 powder was first prepared into a colloidal suspension by dispersing it into a mixed solution of ethanol, polyethylene glycol (PEG) and polyvinyl butyral (PVB) by high energy ball milling using ZrO_2 balls in Turbula equipment for 4 h. The slurry is then cast on a glass support treated beforehand with a mixture of glycerol and ethanol.

The fabrication of the anode-supported half cell began with the preparation of bi-layers of BIT02 electrolyte film on a porous anode substrate by dry co-pressing. The composite powder was first loaded in 13 mm diameter die and pre-formed. The 13 mm diameter electrolyte film, cut into the BIT02 tape, was then loaded in the die on the anode substrate. The bi-layers were co-pressed under a pressure of 90 MPa. The co-pressed pellets were then sintered at 1350 °C for 30 h, resulting in anode-supported configuration. Two cells with different electrolyte thicknesses have been prepared.

The cathode materials $Ba_{0.5}Sr_{0.5}Co_{0.8}Fe_{0.2}O_{3-\delta}$ (BSCF) were synthesized by a glycine nitrate process [57,58]. Required amounts of analytic reagents of $Ba(NO_3)_2$, $Sr(NO_3)_2$, $Co(NO_3)_2{\cdot}6H_2O$, $Fe(NO_3)_3{\cdot}9H_2O$ and $C_2H_5NO_2$, according to the cation stoichiometry of the composite oxide BSCF, were mixed in deionized water to obtain transparent solution. Under stirring and heating at 250 °C, a viscous gel was obtained. When all the water was evaporated, the product was swelled and ignited resulting in porous, foamy and fragile materials. The as-prepared materials were fired at 1000 °C for 16 h in air to obtain pure, well crystallized powder. The cell parameter of the obtained phase ($a = 3.9894(4)$ Å, $Pm\bar{3}m$ space group) refined from XRPD pattern is close to the one reported in the literature ($a = 3.9830(3)$ Å) [59].

The cathode layer was obtained by slurry coating on the electrolyte layer, followed by a sintering at 1200 °C for 10 h. The cathode slurry was prepared according to a method already described in [50].

Current collectors were made from discs (3 mm in diameter) of gold grid (wire diameter 60 μm, grid opening 250 μm) sewed with 50 μm thick gold wired and pasted on both the electrodes using

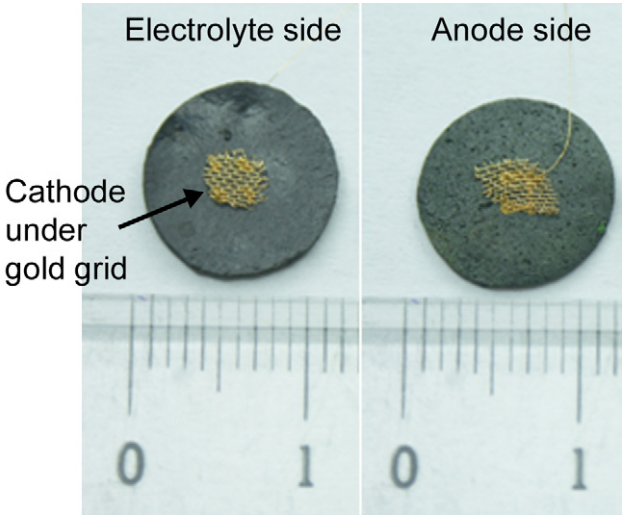

Fig. 2. Front and back images of a complete cell.

gold ink. The cells were then placed in the oven at 140 °C for one night to obtain good electrical and physical contacts (Fig. 2).

2.6. Fuel cells testing

The current–voltage (*I*–*V*) characteristics were measured with the use of a laboratory-made testing system which is schematically represented in Fig. 3. The button cells were pasted using Aremco sealing material (mixture of # 571 L and 571 P) on the top of an alumina sample tube (OD 10 mm, ID 6 mm) thus separating the atmospheres between the inside and outside the tube. The fuel-gas supply tube is located inside the sample tube. The system was kept vertically in a tubular furnace.

Current and voltage measurements were done by digital multimeters Voltcraft MXD-4660A. Current drawn in the circuit was varied using a rheostat. Effective area of the cells in this study was 0.07 cm^2. Cell resistances were determined by swapping the multimeters with a 1250 Frequency Response Analyzer of M/s Solartron (Schlumberger, UK). Measurements were performed at open circuit voltage by using 50 mV of AC perturbation from 63 kHz to 0.1 Hz at 500 °C under wet H_2 flux ($p_{H_2O} = 0.023$ atm).

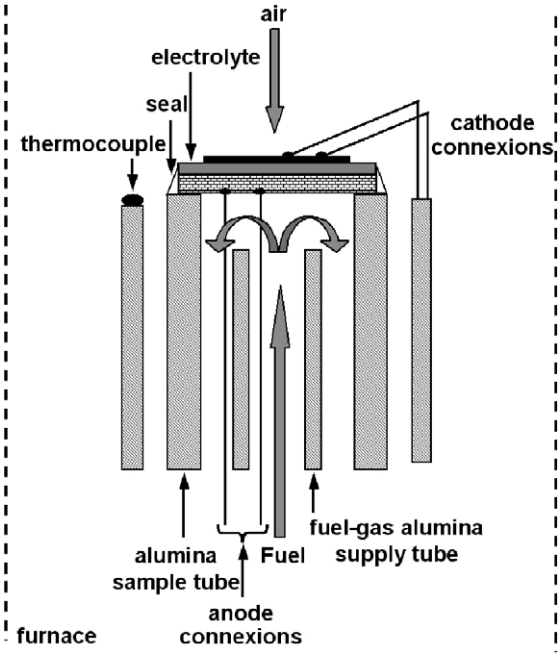

Fig. 3. Schematic view of the cell-testing apparatus.

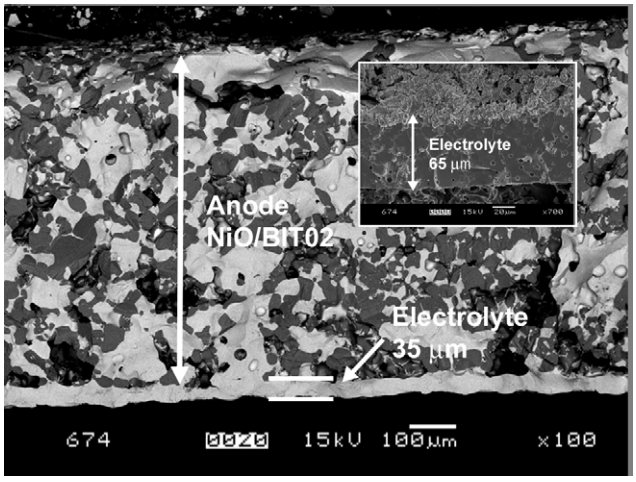

Fig. 4. SEM backscattered electron image of a cross-section on a BIT02/NiO composite and BIT02 tape after sintering showing an electrolyte thickness about 35 µm. The inset shows the SEM secondary electron image for the cell with an electrolyte thickness about 65 µm.

3. Results and discussion

3.1. Electrochemical tests of fuel cells

Fig. 4 shows the SEM micrograph obtained in backscattered electron mode of a transverse section of NiO/BIT02 composite (50 wt.% NiO) and a BIT02 tape after the sintering process. The thickness of the electrolyte is about 35 µm. Both constituents are easily identified. The inset shows the SEM micrograph of the other sintered prepared half cell with a thicker electrolyte and observed with the secondary electron mode. It can be seen that the electrolyte membrane is about 65 µm in thickness and quite dense. The composite was then heated under H_2 5% in Ar flow to determine the reduction temperature of nickel oxide into Ni metal. The reduction is complete after 3 h of treatment at 500 °C (Fig. 5), temperature at which fuel cells with two different electrolyte thicknesses namely 35 and 65 µm were evaluated (denoted afterwards as cell 35 and cell 65).

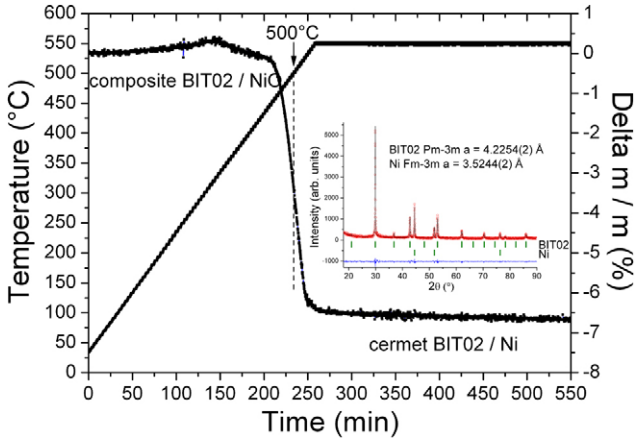

Fig. 5. TGA analysis under H_2 5% in Ar for composite $BaIn_{0.8}Ti_{0.2}O_{2.6}\square_{0.4}$/NiO showing a complete reduction of NiO → Ni after 3 h of treatment at 500 °C. The inset shows the XRD diffraction pattern performed on the TGA residue exhibiting pure BIT02 compound and Ni metal.

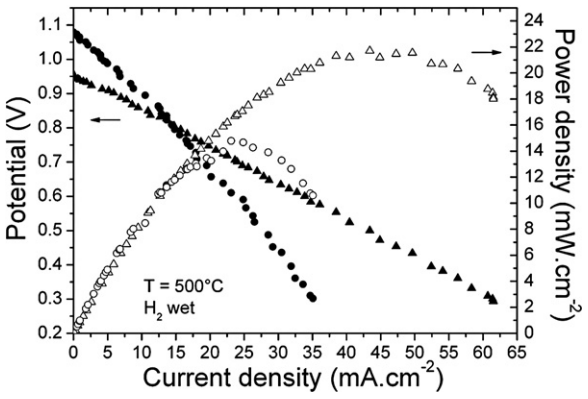

Fig. 6. *I–V* and *I–P* curves recorded at 500 °C under wet H_2 gas ($p_{H_2O} = 0.023$ atm) for both cells: triangles correspond to the cell with an electrolyte thickness about 35 μm and circles for the one with 65 μm electrolyte thickness.

I–V and *I–P* curves of the anode-supported cells are shown in Fig. 6. Measurements recorded in flowing hydrogen gas under wet conditions ($p_{H_2O} = 0.023$ atm) at 500 °C show that the open circuit voltages (OCV) were 0.95 and 1.08 V for the cells 35 and 65, respectively, indicating possibility of small leakage between gas chambers (theoretical value ~1.16 V at 500 °C). The maximum power density reached was, respectively 22 and 15 mW cm^{-2}. The value of the total resistance for the cell 35 calculated from the slope of the whole curve by linear fitting is about 10.7 Ω cm^2 at 500 °C. For the cell 65, two slopes were derived from the curve: the first one starting at the OCV down to the potential 0.85 V gives a total resistance about 17.8 Ω cm^2 and the second one starting from the previous point to 0.30 V gives a total resistance about 23.8 Ω cm^2. The maximum power density at 500 °C is still far from the ones obtained for the anode-supported SOFC based on substituted-$BaCeO_3$ electrolyte (at 500 °C power densities in mW cm^{-2} are 56 [3], 55 [15], 225 [17], 140 [21], 80 [22], 120 [27], 29 [44], 112 [45]) and is in the same order of magnitude as the one obtained in a recent study using $Ba_3Ca_{1.18}Nb_{1.82}O_{9-\delta}$ as electrolyte ($P_{max} \sim 20$ mW cm^{-2} at 500 °C) [23].

Fig. 7 shows impedance spectra measured at 500 °C. The intercept with the real axis at high frequency represents the overall electrolyte resistance, including the resistance of the electrolyte and wires. Obtained values are about 2 and 4 Ω cm^2 for the cell 35 and cell 65, respectively. Assuming the cell resistance mostly comes from the electrolyte, the conductivity of BIT02 membrane for the cell 35 is 1.75×10^{-3} S cm^{-1} at 500 °C that is quite in agreement with the measured conductivity at this temperature (2×10^{-3} S cm^{-1}) [52]. The total interfacial polarization resistance can be determined by subtracting the electrolyte resistance to the total resistance and reached values quite high superior to 8 Ω cm^2 at 500 °C for both cells indicating that the choice of the right cathode materials still remains a challenge for BIT02-based SOFCs. It is noticeable that for the most studied electrolyte proton conductor $BaCe_{1-x}(ZrY)_xO_{3-\delta}$, P_{max} showed by fuel cells based on this material can vary from 120 to 450 mW cm^{-2} independently of the electrolyte thickness showing that the nature, the microstructure of the cathode material and its assembly within the fuel cell play an important role in the performances [3,11,13–16,21,29,30,35,45]. The optimization of these parameters in the BIT02 electrolyte-based fuel cell is under progress.

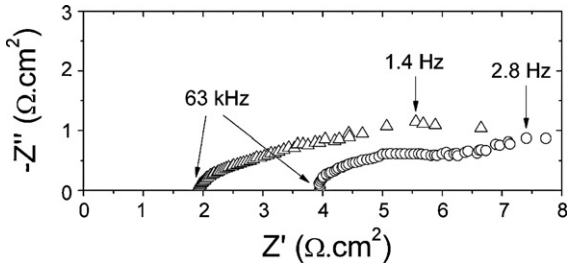

Fig. 7. Impedance spectra of the cells performed under open circuit conditions at 500 °C: electrolyte thickness of 35 μm (triangles) and 65 μm (circles).

4. Conclusion

The present study evaluates the $Ba_2(In_{0.8}Ti_{0.2})_2O_{5.2}$ material as a potential electrolyte material for proton-conducting SOFC. A simple method for fabricating a half cell based on co-pressing of electrolyte tape placed onto anode powder is presented. The electrochemical tests of fuel cells based on BIT02 give at 500 °C under wet H_2 gas for the cell with a 35 μm electrolyte thickness a maximum power density of 22 mW cm^{-2} with an ohmic resistance about 2 Ω cm^2. The contribution of the electrode processes to the total cell resistance is considerable and should be taken into account for further cell improvements: nature of the cathode material, microstructure of the electrodes and assembly of the fuel cells are different parameters to explore. The reduction of the thickness of the electrolyte tape by a factor 2 is another parameter under progress to improve the cell performances.

Acknowledgments

The authors acknowledge the financial support of the French ANR agency through its Tectonic Project managed by M. Marrony from ElfER (ANR-05-PANH-015-03). The authors also would like to thank R. Costa, Centre des Matériaux Mines Paris, France for his collaboration and preparation of BIT02 tapes.

References

[1] Q. Ma, R. Peng, Y. Lin, J. Gao, G. Meng, J. Power Sources 161 (2006) 95.
[2] P. Ranran, W. Yan, Y. Lizhai, M. Zongqiang, Solid State Ionics 177 (2006) 389.
[3] C. Zuo, S. Zha, M. Liu, M. Hatano, M. Uchiyama, Adv. Mater. 18 (2006) 3318.
[4] N. Maffei, L. Pelletier, J.P. Charland, A. McFarlan, J. Power Sources 162 (2006) 165.
[5] K. Xie, Q. Ma, B. Lin, Y. Jiang, J. Gao, X. Liu, G. Meng, J. Power Sources 170 (2007) 38.
[6] Y. Feng, J. Luo, K.T. Chuang, Fuel 86 (2007) 123.
[7] S. Wang, J.-L. Luo, A.R. Sanger, K.T. Chuang, J. Phys. Chem. C 111 (2007) 5069.
[8] Y. Akimune, K. Matsuo, H. Higashiyama, K. Honda, M. Yamanaka, M. Uchiyama, M. Hatano, Solid State Ionics 178 (2007) 575.
[9] L. Bi, S. Zhang, S. Fang, Z. Tao, R. Peng, W. Liu, Electrochem. Commun. 10 (2008) 1598.
[10] L. Bi, S. Zhang, S. Fang, L. Zhang, K. Xie, C. Xia, W. Liu, Electrochem. Commun. 10 (2008) 1005.
[11] B. Lin, S. Zhang, L. Zhang, L. Bi, H. Ding, X. Liu, J. Gao, G. Meng, J. Power Sources 177 (2008) 330.
[12] B. Lin, M. Hu, J. Ma, Y. Jiang, S. Tao, G. Meng, J. Power Sources 183 (2008) 479.
[13] K. Xie, R. Yan, Y. Jiang, X. Liu, G. Meng, J. Membr. Sci. 325 (2008) 6.
[14] K. Xie, R. Yan, D. Dong, S. Wang, X. Chen, T. Jiang, B. Lin, M. Wei, X. Liu, G. Meng, J. Power Sources 179 (2008) 576.
[15] H. Ding, B. Lin, X. Liu, G. Meng, Electrochem. Commun. 10 (2008) 1388.
[16] H. Ding, B. Lin, Y. Jiang, S. Wang, D. Fang, Y. Dong, S. Tao, R. Peng, X. Liu, G. Meng, J. Power Sources 185 (2008) 937.
[17] Y. Lin, R. Ran, Y. Zheng, Z. Shao, W. Jin, N. Xu, J. Ahn, J. Power Sources 180 (2008) 15.
[18] L. Zhang, W. Yang, J. Power Sources 179 (2008) 92.
[19] Z. Shi, J.-L. Luo, S. Wang, A.R. Sanger, K.T. Chuang, J. Power Sources 176 (2008) 122.
[20] E. Fabbri, A. D'Epifanio, E. Di Bartolomeo, S. Licoccia, E. Traversa, Solid State Ionics 179 (2008) 558.
[21] L. Yang, C. Zuo, S. Wang, Z. Cheng, M. Liu, Adv. Mater. 20 (2008) 3280.
[22] H. Matsumoto, I. Nomura, S. Okada, T. Ishihara, Solid State Ionics 179 (2008) 1486.
[23] L. Bi, S. Zhang, S. Fang, L. Zhang, H. Gao, G. Meng, W. Liu, J. Am. Ceram. Soc. 91 (2008) 3806.
[24] A. D'Epifanio, E. Fabbri, E. Di Bartolomeo, S. Licoccia, E. Traversa, Fuel Cells 08 (2008) 69.
[25] T. Wu, R. Peng, C. Xia, Solid State Ionics 179 (2008) 1505.
[26] L. Bi, S. Zhang, B. Lin, S. Fang, C. Xia, W. Liu, J. Alloys Compd. 473 (2009) 48.

[27] L. Bi, S. Zhang, L. Zhang, Z. Tao, H. Wang, W. Liu, Int. J. Hydrogen Energy 34 (2009) 2421.
[28] B. Lin, Y. Dong, S. Wang, D. Fang, H. Ding, X. Zhang, X. Liu, G. Meng, J. Alloys Compd. 478 (2009) 590.
[29] B. Lin, Y. Dong, R. Yan, S. Zhang, M. Hu, Y. Zhou, G. Meng, J. Power Sources 186 (2009) 446.
[30] B. Lin, H. Ding, Y. Dong, S. Wang, X. Zhang, D. Fang, G. Meng, J. Power Sources 186 (2009) 58.
[31] K. Xie, R. Yan, X. Chen, D. Dong, S. Wang, X. Liu, G. Meng, J. Alloys Compd. 472 (2009) 551.
[32] K. Xie, R. Yan, X. Chen, S. Wang, Y. Jiang, X. Liu, G. Meng, J. Alloys Compd. 473 (2009) 323.
[33] K. Xie, R. Yan, X. Liu, J. Alloys Compd. 479 (2009) L40.
[34] K. Xie, R. Yan, X. Liu, J. Alloys Compd. 479 (2009) L36.
[35] Z. Tao, L. Bi, L. Yan, W. Sun, Z. Zhu, R. Peng, W. Liu, Electrochem. Commun. 11 (2009) 688.
[36] M. Zunic, L. Chevallier, F. Deganello, A. D'Epifanio, S. Licoccia, E. Di, E. Bartolomeo, Traversa, J. Power Sources 190 (2009) 417.
[37] S. Zhang, L. Bi, L. Zhang, Z. Tao, W. Sun, H. Wang, W. Liu, J. Power Sources 188 (2009) 343.
[38] K. Xie, R. Yan, X. Xu, X. Liu, G. Meng, J. Power Sources 187 (2009) 403.
[39] B. Lin, S. Wang, X. Liu, G. Meng, J. Alloys Compd. 478 (2009) 355.
[40] L. Bi, Z. Tao, W. Sun, S. Zhang, R. Peng, W. Liu, J. Power Sources 191 (2009) 428.
[41] R.T. Baker, R. Salar, A.R. Potter, I.S. Metcalfe, M. Sahibzada, J. Power Sources 191 (2009) 448.
[42] E. Fabbri, S. Licoccia, E. Traversa, E.D. Wachsman, Fuel Cells 09 (2009) 128.
[43] K. Xie, R. Yan, X. Xu, X. Liu, G. Meng, Mater. Res. Bull. 44 (2009) 1474.
[44] L. Bi, S. Fang, Z. Tao, S. Zhang, R. Peng, W. Liu, J. Eur. Ceram. Soc. 29 (2009) 2567.
[45] Y. Guo, Y. Lin, R. Ran, Z. Shao, J. Power Sources 193 (2009) 400.
[46] T. Wu, Y. Zhao, R. Peng, C. Xia, Electrochim. Acta 54 (2009) 4888.
[47] V. Jayaraman, A. Magrez, M. Caldes, O. Joubert, M. Ganne, Y. Piffard, L. Brohan, Solid State Ionics 170 (2004) 17.
[48] T. Delayahe, O. Joubert, M.-T. Caldes, Y. Piffard, P. Stevens, Solid State Ionics 177 (2006) 2945.
[49] D. Prakash, T. Delayahe, O. Joubert, M.-T. Caldes, Y. Piffard, P. Stevens, ECS Trans. 7 (2007) 2343.
[50] D. Prakash, T. Delahaye, O. Joubert, M.-T. Caldes, Y. Piffard, J. Power Sources 167 (2007) 111.
[51] V. Jayaraman, A. Magrez, M. Caldes, O. Joubert, F. Taulelle, J. Rodriguez-Carvajal, Y. Piffard, L. Brohan, Solid State Ionics 170 (2004) 25.
[52] E. Quarez, S. Noirault, M.-T. Caldes, O. Joubert, J. Power Sources 195 (2010) 1136.
[53] J. Will, A. Mitterdorfer, C. Kleinlogel, D. Perednis, L.J. Gauckler, Solid State Ionics 131 (2000) 79.
[54] F. Tietz, H.-P. Buchkremer, D. Stöver, Solid State Ionics 152 (2002) 373.
[55] K.C. Wincewicz, J.S. Cooper, J. Power Sources 140 (2005) 280.
[56] H. Moon, S.D. Kim, S.H. Hyun, H.S. Kim, Int. J. Hydrogen Energy 33 (2008) 1758.
[57] R.D. Purohit, S. Saha, A.K. Tyagi, J. Nucl. Mater. 288 (2001) 7.
[58] B. Liu, Y. Zhang, J. Alloys Compd. 453 (2008) 418.
[59] H. Koster, F.H.B. Mertins, Powder Diffr. 18 (2003) 56.